RAMReS Sciences des Structures et de la Matière Vol. 9, N°2 (2025) 22 - 39
http://publication.lecames.org/index.php/mat ISSN: 2630-1180

A Channel quality prediction approach for a commercial Multiband Mobile Network

Ndolane Diouf[1,*], Massa Ndong[2], Mamadou Sarr[1], Dialo Diop[1], Kharouna Talla[1]

[1]*Faculty of Sciences and Technologies, Cheikh Anta Diop University, Dakar, Senegal*
[2]*Science, Technology and Digital Division, Cheikh Hamidou Kane Digital University, Dakar, Senegal*

Received: 11 May 2025 / Received in revised form: 11 September 2025 / Accepted: 05 October 2025

***Abstract*:**

Accurately predicting wireless channel quality is crucial for enabling mobile network operators to carry out proactive network operations. In this article, we address the challenge of predicting channel quality across various wireless links. Building on our previous work, we introduce two new models: a Convolutional Neural Network (CNN) and a hybrid CNN-LSTM, which combines CNN with a Long Short-Term Memory (LSTM) architecture. These models are designed to predict the Channel Quality Indicator (CQI) in 4G LTE/5G networks incorporating small cell base station architectures. We evaluate their performance using a dataset collected from Orange Senegal's commercial 4G LTE/5G network. Our results demonstrate that the CNN, LSTM, and CNN-LSTM models adapt effectively to real-world conditions and achieve high prediction accuracy. Among them, the CNN-LSTM model delivers the best performance (RMSE = 0.25), followed by the LSTM model (RMSE = 0.281), and the CNN model (RMSE = 0.308).

***Keywords*:** Dataset; CQI; Small cell mobile network; 4G LTE/5G; CNN-LSTM.

1. Introduction

Fourth-generation (4G) and fifth-generation (5G) cellular networks currently represent the dominant mobile technologies worldwide. Analyzing network behavior can help predict traffic patterns and improve network performance [1]. Accurately anticipating channel conditions enables proactive optimization of wireless communication systems. Predicting the state of a radio channel in a mobile network relies on historical channel information to forecast its future condition. In our study, prediction involves multiple wireless channels across LTE (Long-Term Evolution)

* Corresponding author:
Email address: *ndolane.diouf@ucad.edu.sn (N. Diouf)*
https://doi.org/10.70974/mat0922522

cells operating on different frequency bands (i.e., 1800 MHz and 2100 MHz). The Channel Quality Indicator (CQI) serves as the key performance indicator used to assess channel conditions, supporting adaptive modulation and coding. It is a key parameter that helps improve throughput and transmission efficiency based on signal quality. Reported CQI values range from 0 to 15, with higher values reflecting better channel conditions and the potential for higher transmission rates [2]. In our previous work [3], we investigated the relationship between CQI and perceived downlink throughput. We demonstrated that CQI is the variable with the greatest influence on the throughput experienced by users in a 4G LTE/5G network and that it predicts this throughput with significantly higher accuracy. In our work [4], we used deep neural networks (DNNs) and LSTM to predict channel quality in a small-cell 4G LTE/5G mobile network.

Several research studies have proposed different radio channel estimation strategies. The authors of [5] propose a deep learning-based channel estimation and tracking algorithm for vehicular millimeter wave communications. In [6], the authors develop a deep learning (DL)-based method for estimating channel responses in vehicle-to-vehicle and vehicle-to-infrastructure (V2I) communications. The authors of [7] propose a real-time radio channel prediction algorithm based on a convolutional neural network (CNN). In [8], the authors use a mixed CNN-LSTM model to predict LTE and 5G channel profiles. Further details on channel estimation can be found in [9–12].

In this article, we propose a CNN and a hybrid CNN-LSTM model for CQI estimation. The mobile dataset used for the experimental part of this study was collected from the 4G LTE/5G radio access network of Orange Senegal. The measurement campaigns span a period of over three months. Specifically, we identify several features that affect the CQI of a radio link, and each data sample consists of information related to these features and the corresponding CQI. In our study, it is important to clarify how CQI values, which range from 0 to 15, are utilized by our deep learning models. CQI is inherently a discrete variable encoded on 4 bits according to the 3GPP standard, representing a qualitative measure of channel conditions and serving as the basis for MCS (Modulation and Coding Scheme) adaptation. We adopt a regression-based approach in which CQI is treated as an ordinal continuous variable within the range [0, 15], and our CNN and CNN-LSTM models are trained to predict a numerical value. In our experimental framework, the models are designed to predict CQI as a normalized numerical value in the interval [0, 1], which is then mapped back to the discrete scale [0, 15] for final evaluation. This hybrid approach (regression + discretization) enables us to leverage the continuous RMSE (Root Mean Square Error) metric to assess prediction accuracy while preserving the ordinal nature of CQI for operational interpretation within the network.

The rest of this article is structured as follows: Section 2 gives the problem statement and background. The hardware, deep learning models, and method are detailed in Section 3. We then present the results and discussion in Section 4, and conclude the paper in Section 5.

2. Problem Statement and Background

In this paper, we propose a deep learning (DL) approach to predict the quality of wireless channels in 4G LTE/5G small cell networks. We focus on a reference scenario involving six small cell base stations (SBSs). Two SBSs are deployed at each of three different sites with distinct sectors. The network comprises multiple LTE cells operating on two frequency bands (i.e., 1800 MHz and 2100 MHz).

SBSs are cellular systems deployed in an area covered by an MBS (Macro Base Station) to improve spectrum efficiency. SBSs operate on the same frequency band

as MBSs but are used in areas where MBS coverage is weak. By connecting more users to SBSs, operators can increase the utilization of the frequency band in a given area. The design of SBS integration into MBSs remains a key consideration in 5G and beyond, as defined by the 3GPP (Third Generation Partnership Project) standard [13].

SBS architecture is particularly relevant in the context of CQI prediction, as it introduces greater channel variability than MBSs. Due to their limited coverage radius, SBSs are deployed in urban environments with high user density, where propagation conditions are strongly influenced by obstacles, multiple reflections, and multipath phenomena. In addition, user load fluctuates greatly in these environments, leading to rapid variations in radio resource allocation. Unlike MBSs, where propagation conditions are more stable and homogeneous, SBSs therefore pose more complex predictive challenges but offer an ideal setting for testing the effectiveness of deep learning models capable of capturing these subtle dynamics. Finally, frequency reuse between SBSs and MBSs can generate additional local interference, further complicating prediction. Thus, while SBSs are an ideal testing ground for developing and testing advanced predictive models, they also pose more demanding methodological challenges related to the intrinsic complexity and variability of the channel.

Our goal is to predict the downlink wireless channel CQI (Channel Quality Indicator) at a given frequency, using data collected from the access network of Orange Senegal, which comprises six SBSs. Fig. 1 illustrates the SBS deployment scenario at the Massalikoul Djinane complex.

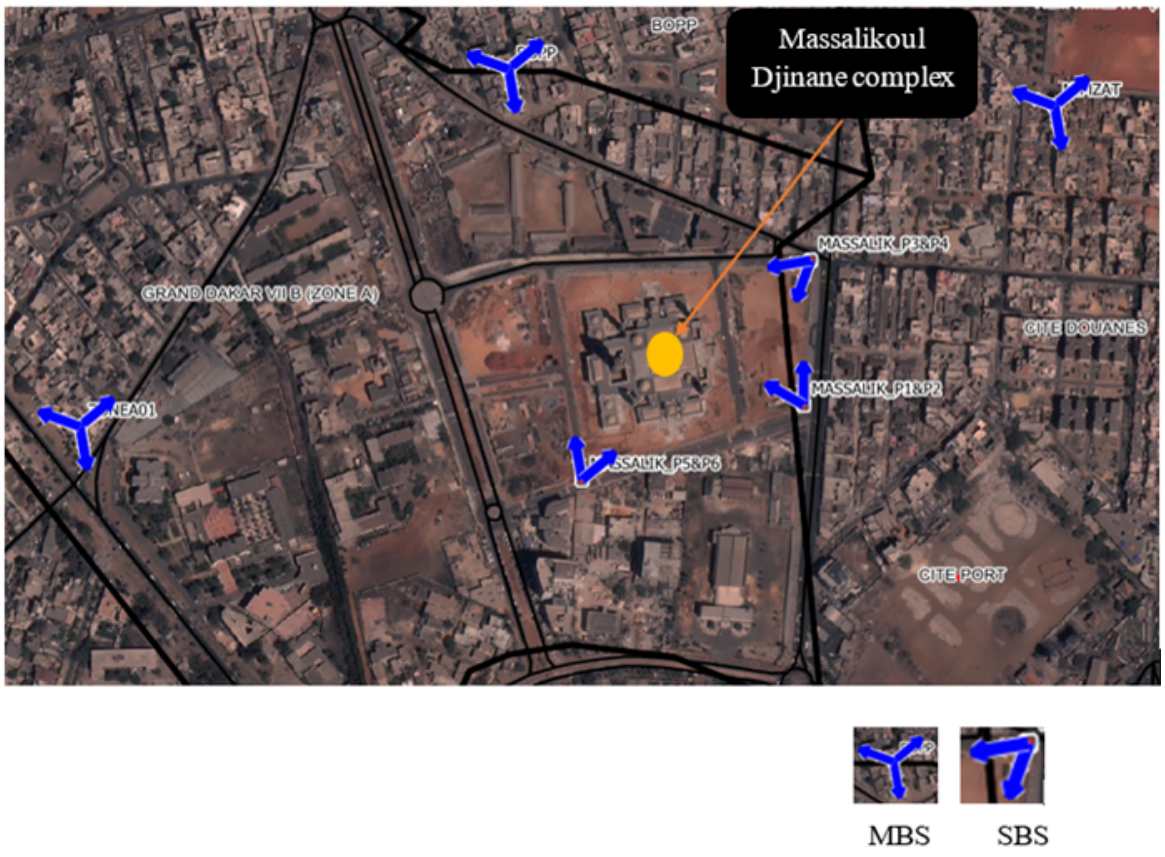

Fig. 1. The deployment scenario of SBSs around the Massalikoul Djinane complex.

3. Materials, Deep Learning Models, and Methods

3.1. Materials

In this article, a framework for predicting channel quality in 4G LTE/5G networks using DL models is structured into three main steps: (i) data collection, (ii) data preprocessing, and (iii) training, testing, and evaluating DL models. The multistep framework is illustrated in Fig. 2. The proposed approach requires effective data collection for both training and validation purposes. Next, the data undergoes clustering and feature selection based on feature correlation. Finally, DL models are applied to predict the CQI, and the results are compared with real-world data for validation, in order to identify the optimal DL model.

3.1.1. 4G LTE/5G Data Collection

The dataset was collected from Orange Senegal's commercial 4G LTE/5G radio access network. Data collection involved six SBSs and took place in an urban environment within the Grand Dakar district, specifically around the Massalikoul Djinane complex, located in the south-central part of the Senegalese capital. The data spans a period of over three months, from August 3, 2020, to November 10, 2020. All data was gathered under consistent weather conditions. Fig. 3 illustrates the data collection process. For simplicity in the data collection diagram, we employed three MBS and three SBS.

The characteristics of the antenna used for data collection are detailed in Table 1.

3.1.2. Dataset

Real-world data composed of Key Performance Indicators (KPIs) is used for CQI prediction by applying selected DL models. These indicators enable mobile network operators to monitor and optimize the performance of their networks where necessary. This dataset is crucial for analyzing and optimizing mobile network performance, ultimately contributing to an improved user experience. Figure 4 illustrating the correlation between different KPIs in our dataset highlights the relevance of the 12 selected KPIs for CQI prediction. We first observe a strong interdependence between traffic-related KPIs (DL_Traffic, Traffic_UL, Total_Traffic) and radio resource occupancy indicators (DL_PRB_Rate, UL_PRB_Rate). This logically reflects the impact of network load on spectral availability, and consequently, on channel quality. The number of connected users (Active_user_Max, RRC_user_Max) shows a moderate correlation with CQI, indicating the influence of user density on resource sharing. Conversely, KPIs such as CDR and Radio_DL_Delay_avg display, respectively, a weak positive and a negative correlation with CQI, confirming that degraded radio conditions result in lower perceived quality. Meanwhile, user throughput KPIs (Throughput_UL_user, Throughput_DL_user, DL_perceived_throughput) exhibit notable positive correlations with CQI, underlining the direct relationship between radio quality and effective transmission capacity. Taken together, these observations justify the selection of our 12 features, as they complementarily capture network load, resource utilization, radio quality, and user experience, thus providing a solid foundation for CQI modeling and prediction in 4G LTE/5G cellular networks. The definition of each feature or KPI is provided as follows:

- **DL_Traffic (GB):** This refers to the average daily downlink data traffic per cell for all users.
- **UL_Traffic (GB):** This refers to the average daily uplink data traffic per cell for all users.
- **Total_Traffic (GB):** This represents the total amount of data traffic (uplink + downlink).
- **Active_user_Max:** This indicates the maximum number of active users.
- **RRC_user_Max:** This represents the maximum number of RRC (Radio Resource Control) connected users.

- **Throughput_UL_user (Kbit/s):** This indicates the uplink throughput per user.
- **Throughput_DL_user (Kbit/s):** This indicates the downlink throughput per user.
- **DL_PRB_Rate:** This denotes the rate of physical resource block (PRB) used in the downlink.
- **UL_PRB_Rate:** This denotes the rate of physical resource block (PRB) used in the uplink.
- **CDR (Call Drop Rate):** This indicates the call drop rate.
- **CQI:** Represents the channel quality indicator.
- **Radio_DL_Delay_avg:** This indicates the average downlink delay over the 4G LTE radio access network.
- **DL_perceived_throughput (Mbps):** This refers to the perceived downlink throughput.

A sample of the raw data collected from the 4G LTE/5G network is shown in Table A1 in Appendix.

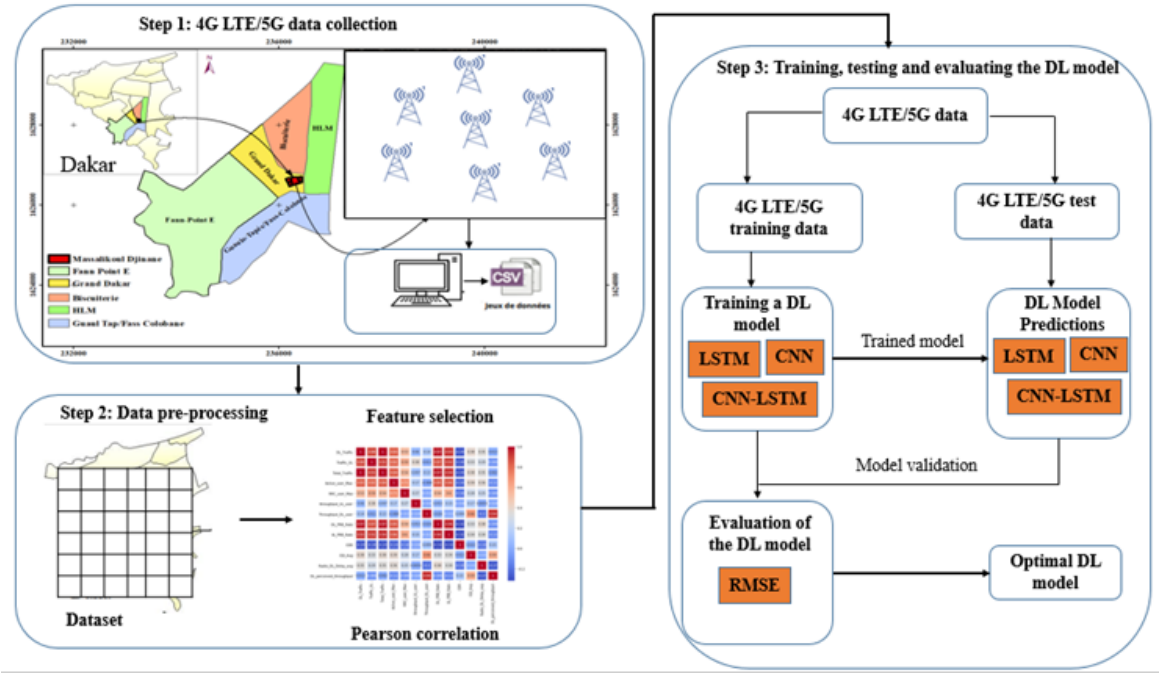

Fig. 2. Multi-step framework for channel quality indicator prediction.

Table 1
Characteristics of the antenna used for data collection.

Parameters	Specifications
Frequency band	1800 MHz, 2100 MHz
Radio access technology	LTE, UMTS, GSM
Power	2 × 60 W
Size	750 mm × 165 mm
Weight	17 kg
Current source	DC/AC/DC 240 V

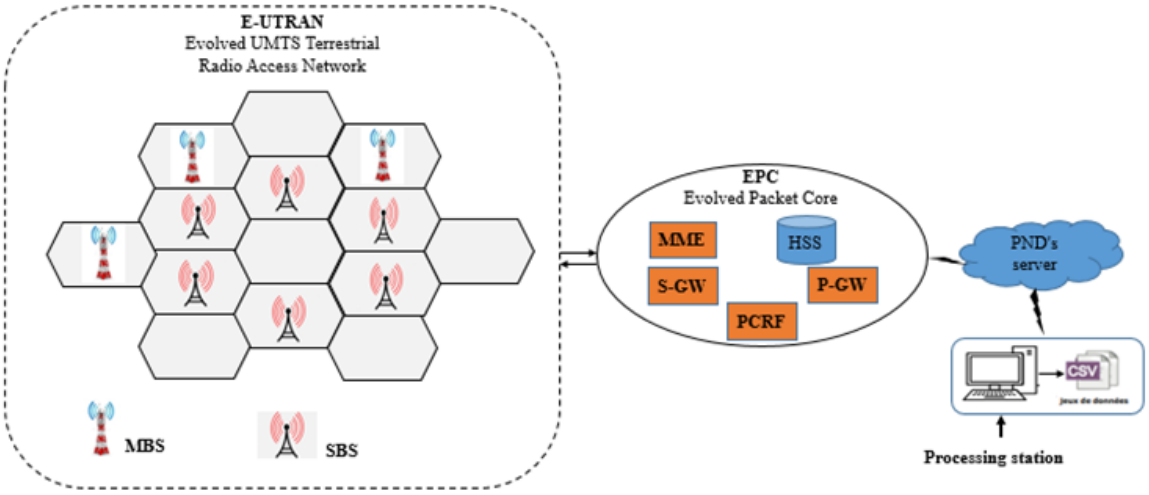

Fig. 3. The diagram illustrating data collection.

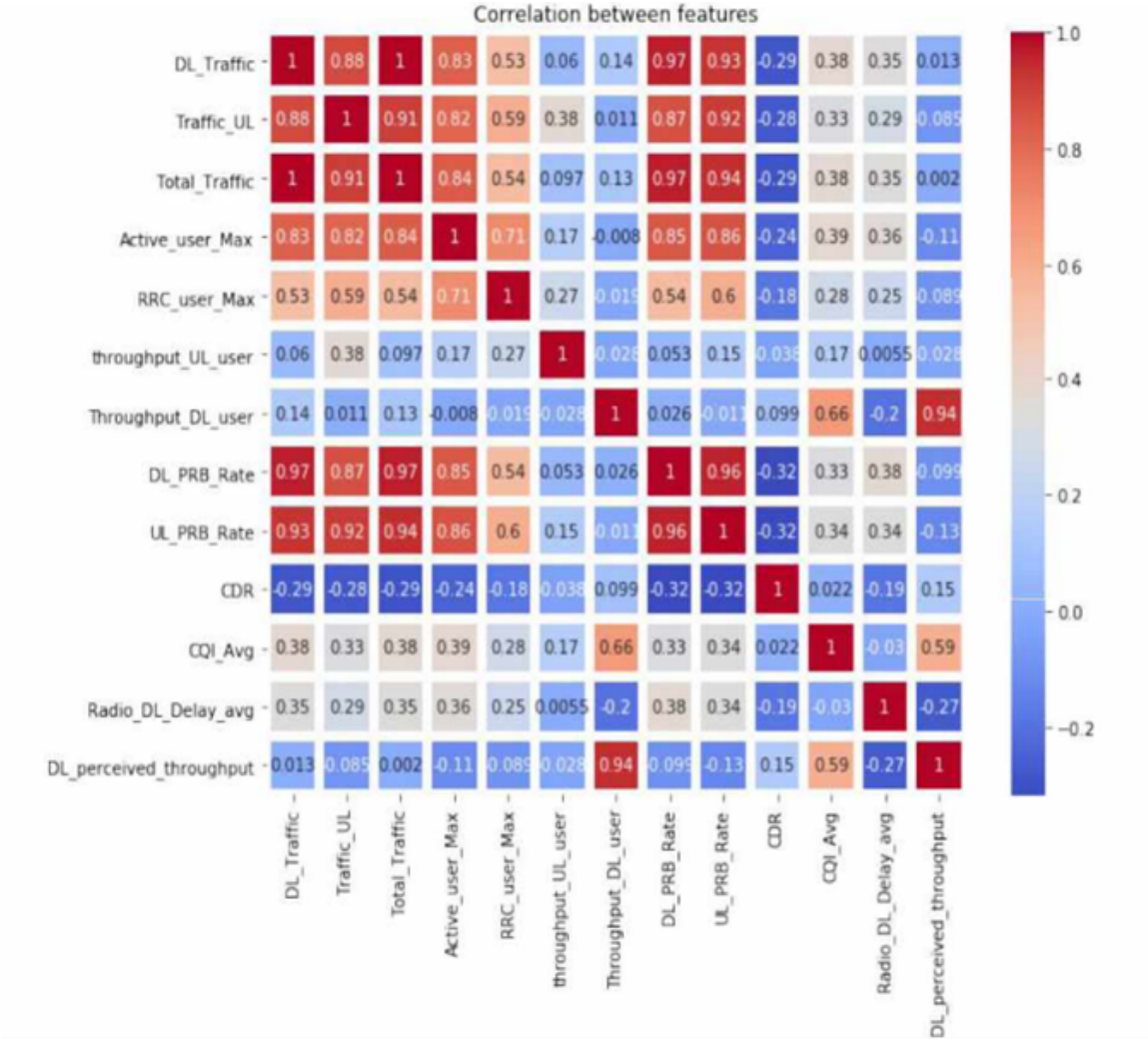

Fig. 4. Correlation between dataset characteristics.

3.1.3. Data Preprocessing

Artificial neural networks may not perform correctly without proper preprocessing of input data. After the data collection stage, we obtain raw data that cannot be directly used by deep learning models. This raw data often contains different measurement units, missing values, and outliers. Therefore, we applied preprocessing

techniques to the raw data to reduce challenges and ensure both accuracy and efficiency during the prediction phase.

Data preprocessing involves: (i) handling missing values, (ii) feature scaling, (iii) reducing redundancy through dimensionality reduction, and (iv) removing outliers.

Handling missing values is a crucial step in training neural networks. This stage helps prevent the model from making errors in its predictions. In this study, we identified these missing values. Thus, after identifying all the missing values in each column, we replaced each missing numeric value with the mean of its respective column.

Scaling features to the same range generally enables the deep learning model to better identify distinct patterns in the dataset. One reason this is important is that features are multiplied by the model's weights; thus, the scale of both outputs and gradients is influenced by the scale of the inputs. The data collected for this study includes variables measured in different units. Therefore, we applied scaling to bring all variables onto the same scale. We used the appropriate min-max scaling technique to transform the dataset into the [0, 1] range. The formula we used for data scaling is given in [14] and is expressed as follows:

$$z_i = \frac{x_i - \min(x)}{\max(x) - \min(x)} \qquad (1)$$

Where $x = (x_1, \ldots, x_n)$ represents the original data, z_i is the i-th data point after scaling, and $\min(x)$ and $\max(x)$ are respectively the smallest value (score of 0) and the largest value (score of 1) of the original data.

However, selecting all available variables in a dataset is not always the best option, as it may lead to poor predictions. Feature selection is a critical part of the preprocessing phase in data compression, which involves dividing the dataset into more meaningful and manageable groups. Choosing the right features is essential for identifying relevant and useful information for the DL training phase, while filtering out irrelevant data points. Various feature selection methods are used, and in this work, Pearson correlation was applied to test the dependency between parameters within the dataset. Correlation coefficients range from -1 to +1: values close to +1 indicate a strong positive linear correlation, values near zero suggest a weak correlation, and values close to -1 indicate a strong negative correlation [15]. The Pearson correlation coefficient is calculated as follows:

$$\rho = \frac{\sum_{i=1}^{n}(x_i - \bar{x})(y_i - \bar{y})}{\sqrt{\sum_{i=1}^{n}(x_i - \bar{x})^2 \sum_{i=1}^{n}(y_i - \bar{y})^2}} \qquad (2)$$

Where x_i are the values of variable **x** in a sample, $\bar{x}$ is the mean of the values of variable x, y_i are the values of variable y in a sample, and $\bar{y}$ is the mean of the values of variable y.

Outliers are data points that are either insignificant or markedly different from the rest of the dataset. We applied the statistical Interquartile Range (IQR) method, where values falling outside the interval [Q1 - 1.5×IQR, Q3 + 1.5×IQR] are classified as outliers [16]. Handling outliers is crucial in prediction tasks, since a deep learning model that attempts to fit them may suffer degraded performance on other, more relevant data points. Therefore, in this study, we addressed outliers using an imputation approach, where each outlier was replaced with the mean of its neighborhood [17]. Fig. 5 shows the distribution of features in our dataset after normalization.

3.2. Deep Learning Models

DL uses multiple layer architectures to extract features at different levels of abstraction from raw data. The classic supervised learning approach needs features and labels. For this purpose, DL_Traffic (GB), Traffic_UL (GB), Total_Traffic (GB), Active_user_Max, RRC_user_Max, Throughput_UL_user (Kbps), Throughput_DL_user (Kbps), DL_PRB_Rate, UL_PRB_Rate, CDR, Radio_DL_Delay_avg, DL_perceived_

throughput (Mbps) are used as features and inputs of our two models. CQI is the label for LSTM, CNN and hybrid CNN-LSTM models. The architecture of each model is explained below.

LSTM Model Architecture: Our network architecture for the simulation features densely connected sequential layers with ReLU activation functions as neurons. The architecture is composed of an input layer, 3 hidden layers, and an output layer. Our LSTM is designed such that the information goes through a loop, which allows it to consider the current input and also what it has learned from the inputs it has received previously when making a decision. The root mean square error between the predicted CQI and the measured CQI was minimized during the training process with the Adam optimizer. In sequence prediction problems, it is able to learn order dependence [18]. The LSTM architecture is shown in Fig. 6.

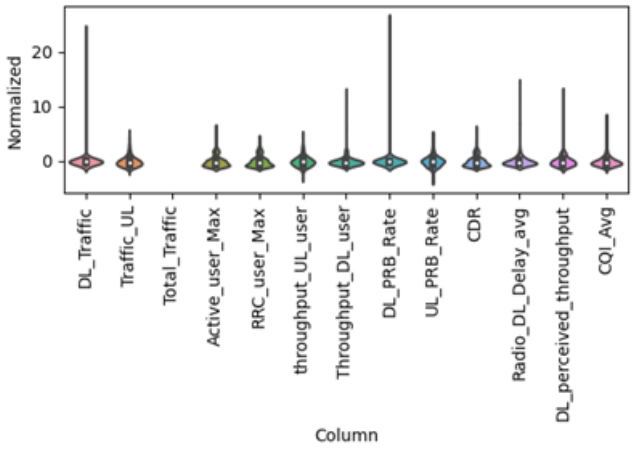

Fig. 5. Feature distribution after normalization.

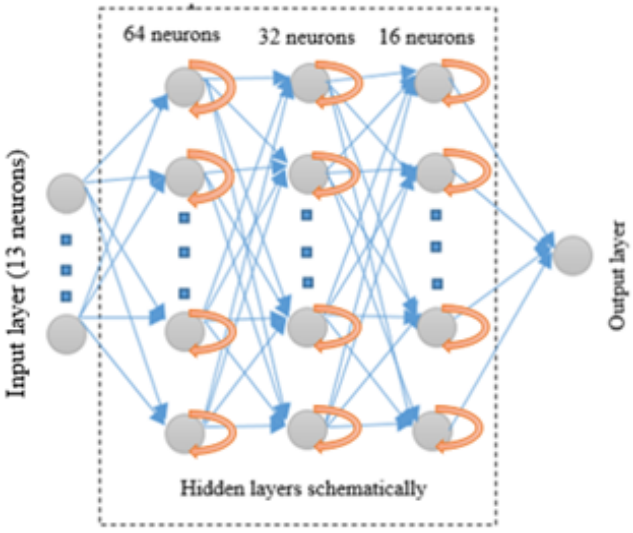

Fig. 6. Proposed LSTM architecture for CQI prediction.

Difference between DNN and LSTM Models: In a deep neural network (DNN), information flows in only one direction: from the input layer, through the hidden layers, to the output layer. In contrast, in an LSTM, information loops back on itself. When making a decision, it considers both the current input and what it has learned from previous inputs. A DNN has no memory of past inputs and is therefore poor at predicting what comes next. It retains nothing from the past except what it learned during training. LSTM, on the other hand, can remember their inputs over long periods of time. This is because the LSTM keeps its information in memory, which is very similar to computer memory because the LSTM can read, write, and delete information from its memory. Deep learning has the ability to learn features at multiple levels of abstraction for a dataset. It allows a system to learn complex features and match input to output directly from the data [19]. The deep learning architecture is flexible to be adapted to new problems in the future [20], such as the case of CQI prediction in this paper. Figure 7 below illustrates the difference in information flow between an LSTM and a DNN.

CNN Architecture: The architecture of our CNN model is a combination of several identical CNNs. We have placed MaxPooling1D layers after each convolutional layer. The main objective of the MaxPooling1D layer is to reduce the size of the feature maps, which speeds up computation as the number of training parameters is reduced. All the 2-dimensional arrays resulting from the feature aggregation are converted into a single linear vector by the Flatten layer. Dense layers are used for final prediction. This is because dense layers are able to capture complex patterns in the data and learn the relationships between different parts of the input. We use ReLU as the activation function. The CNN architecture is shown in Fig. 8.

CNN-LSTM Architecture: The hybrid CNN-LSTM model leverages the complementary strengths of convolutional and recurrent networks for CQI prediction in 4G LTE/5G systems. First, the Conv1D layers combined with MaxPooling act as local feature extractors by automatically identifying salient patterns within the time sequences of radio KPIs (inputs). This step reduces data complexity while better capturing rapid channel variations, particularly those caused by fading and interference. The extracted representations are then passed to the LSTM layer, whose memory units can model long-term temporal dependencies and the evolving dynamics of the radio channel. This capability is critical in 4G LTE/5G environments, where user mobility, multipath variability, and network load significantly affect link quality. The sequential output of the LSTM is flattened and forwarded to a fully connected layer. Finally, the fully connected layers exploit these enriched sequential representations to accurately predict CQI, thereby enabling more effective adaptation of the modulation and coding scheme (MCS) and contributing to the optimization of radio resource allocation. The CNN-LSTM architecture is shown in Fig. 9.

We defined the CNN and CNN-LSTM architectures using optimal hyperparameters. To avoid redundancy when describing architectures with 4, 5, or 6 layers, we chose to present only a single representative architecture for each model. Consequently, instead of detailing six distinct architectures across both models (CNN and CNN-LSTM), we presented two representative ones for clarity and conciseness.

The choice of hyperparameters was driven by the need to ensure both stability and generalization of our models. The Adam optimizer with a learning rate of 0.0005 was selected for its fast and robust convergence on our mobile data.

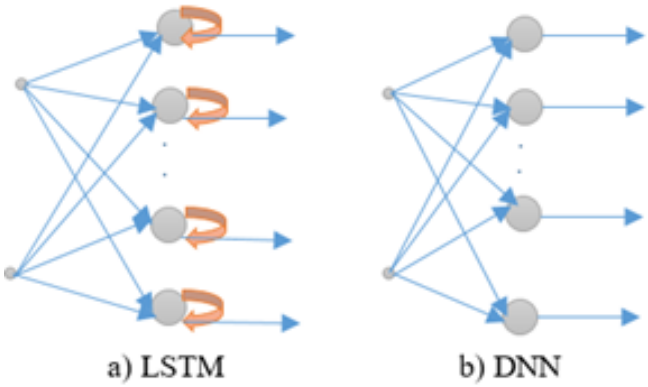

Fig. 7. Difference between LSTM and DNN architectures.

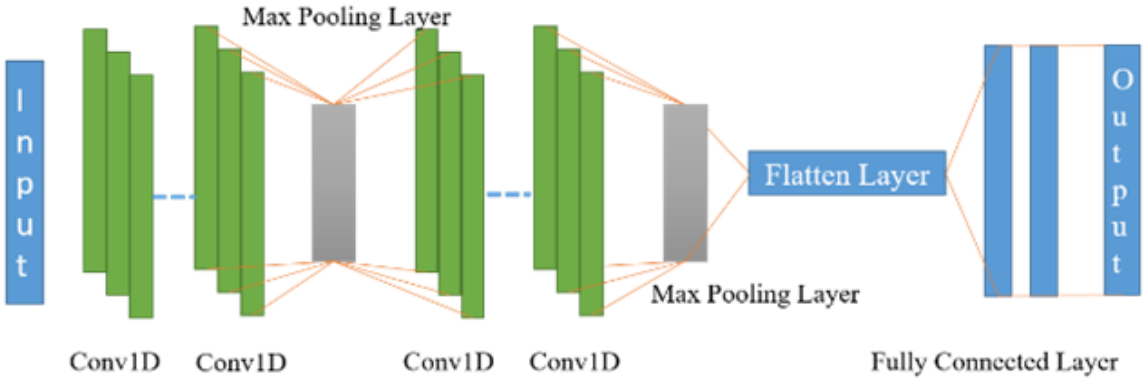

Fig. 8. Proposed CNN architecture for CQI prediction.

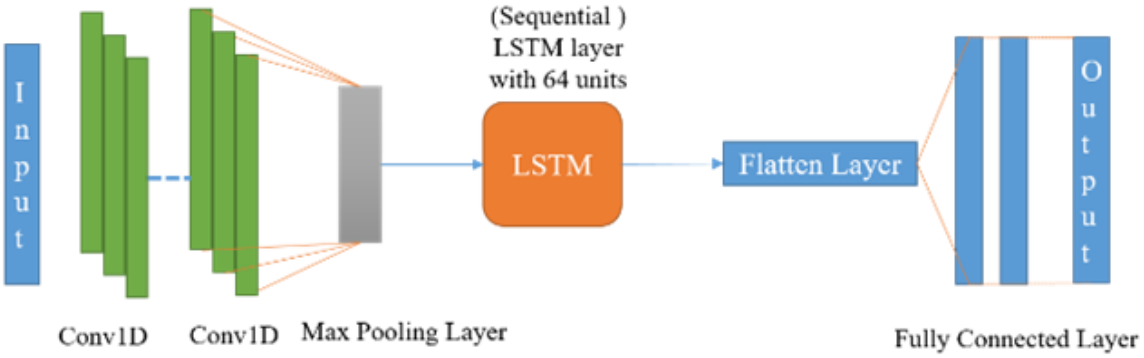

Fig. 9. Proposed CNN-LSTM architecture for CQI prediction.

The Mean Squared Error (MSE) loss function was chosen given the nature of the task, which consists of continuous CQI regression. The batch size was set to 32, providing a balance between gradient stability and GPU memory constraints. Training was limited to 100 epochs to guarantee optimal convergence of each model. The Rectified Linear Unit (ReLU) activation function was adopted in the architecture of all our models due to its favorable properties for deep learning. It enables the models to capture complex nonlinear relationships while ensuring efficient and stable training. The number of layers determines the hierarchical depth of the model's learning. This allows the model to progress from detecting simple features to more complex abstract representations. This is essential for accurate CQI prediction in spatiotemporal environments such as 4G LTE/5G networks.

Simulation hyperparameters for CNN, LSTM, and CNN-LSTM architectures are collected in Table 2.

Table 2
Training Hyperparameters.

Hyperparameters	CNN	LSTM	CNN-LSTM
Batch Size	32	32	32
Number of epochs	100	100	100
Number of layers	4, 5, 6	4, 5, 6	4, 5, 6
Activation function	ReLU	ReLU	ReLU
Optimizer	Adam	Adam	Adam
Loss	Mean squared error	Mean squared error	Mean squared error
Learning rate	0.0005	0.0005	0.0005

3.3. Predictive Methodology

In this part, we seek to predict the CQI, which represents our target variable. Thus, all the other variables represent the independent ones. To perform the prediction, we use DL models such as LSTM, CNN, and CNN-LSTM.

After preprocessing the data, we divide the dataset into two subsets. Accordingly, 90% of the data are allocated to the training set, while the remaining 10% are reserved for the test or validation set. Our CNN model, and particularly the hybrid CNN_LSTM architecture, involve a large number of parameters. The CNN learns spatio-temporal patterns constructed from KPI windows, while the CNN_LSTM extends this by incorporating recurrent cells to explicitly capture long-term temporal dependencies. These characteristics explain why allocating 90% of the observations to training is beneficial: it supports robust estimation of the many parameters, enables the discovery of rare patterns, and helps reduce the risk of overfitting. Moreover, our dataset is a time series characterized by autocorrelation and seasonality. Consequently, the split is chronological: we used the earliest 90% of the data for training, applying internal chronological validation (walk-forward cross-validation). The remaining 10% of the data were reserved for model validation. This approach prevents temporal information leakage and mirrors the operational setting, where the goal is to forecast the future based on the past. Fig. 10 visualizes all training and test data. We use variables from the training set as input for the models. Finally, we use the model trained with variables from the test set to predict the CQI, i.e., the CQI in the test set.

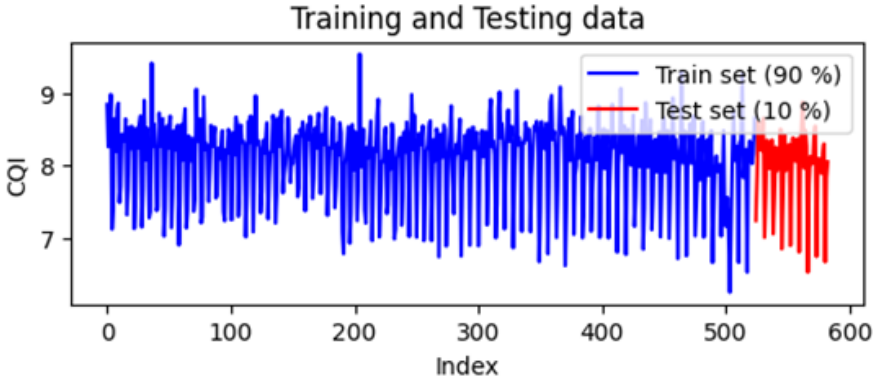

Fig. 10. Distribution of training and testing datasets.

4. Numerical Results and Discussion

In this section, we discuss the performance of CQI predictions with LSTM, CNN, and CNN-LSTM models. To demonstrate the performance of our different models, we compare the prediction results during the training and testing processes with the ground truth (i.e., the measured CQI). The prediction accuracy is measured by the root mean squared error (RMSE) between real and predicted values in the test set (with size $T_{\text{test}} = N$) defined by Equation 3:

$$RMSE = \sqrt{\frac{1}{N}\sum_{i=1}^{N}(A_i - P_i)^2} \qquad (3)$$

Where A_i is the i-th value of CQI in the test set, P_i is the i-th corresponding predicted value of CQI, and N is the number of CQI observations in the test set. RMSE is preferable to MAE when outlier behavior is large as is the case in our study. Moreover, the RMSE metric is more suitable than the MAE, since RMSE penalizes large prediction errors more heavily. In fact, in a 4G LTE/5G network, a significant underestimation or overestimation of the CQI can negatively impact both Quality of Service (QoS) and spectral efficiency. Unlike MAE, which treats all errors linearly, RMSE squares the deviations before averaging them, thereby amplifying the influence of large errors. This makes it possible to more rigorously assess the model's ability to deliver reliable predictions under the most adverse channel conditions (severe fading, interference, high mobility).

After implementing the models, we use a training and testing or validation data set to measure the performance of each model. Thus, the RMSE metric is used to see training and validation losses. Fig. 11 shows the performance of training loss and test values for CQI values with the number of epochs.

As Fig. 11 shows, the training loss decreased with increasing number of epochs. The training loss quickly converges to a low value of 0.15. Since the error on the validation set closely matches the training set, the network did not overfit the training data with the validation values.

The prediction performance of each deep learning (DL) algorithm is evaluated on a set of test data. The predicted values of CQI versus the actual values in the data set are plotted in Fig. 12 for LSTM, CNN, and CNN-LSTM models. As Fig. 12 shows, the actual and predicted CQI values approximate or are plotted similarly. Therefore, the proposed CNN, LSTM, and CNN-LSTM models can easily adapt and make an efficient prediction with the actual values. The RMSE performance of each of the new CNN and CNN-LSTM models is compared to that of our LSTM model presented in [4]. Thus, we varied the number of layers for each model to obtain different RMSEs. This allows us to compare performance between models. The performance of each model in predicting the CQI is presented in Table 3. The dataset is from 4G mobile data Orange Senegal.

Table 3
Performance evaluation (RMSE values).

	Number of layers		
	4	5	6
CNN	0.303	0.288	0.308
LSTM	0.303	0.270	0.281
CNN–LSTM	0.304	0.262	0.250

Analysis of the results in Table 3 shows that our new CNN-LSTM model is better than the reference LSTM and CNN model, because it gives a lower RMSE (i.e., RMSE equal to 0.25 for a number of layers equal to 6). CQI does not have a physical unit because it is a dimensionless index, represented by an integer value between 0 and 15 in the LTE/5G standard. The unit of the RMSE metric always depends on that of the predicted variable, which in this case is CQI, so the RMSE of CQI is also dimensionless.

The statistical results of Table 3 are shown graphically in Fig. 13. This figure shows the different RMSE values for each of the CNN, LSTM, and CNN-LSTM models.

Fig. 13 shows that the performance of the CNN-LSTM model improves as the number of layers increases. In the literature, a lower RMSE value indicates fewer errors and thus better model performance. Based on the collected data, the CNN-LSTM model outperforms our LSTM model presented in [4].

4.1. The Limitations of CNN and CNN-LSTM Models in CQI Prediction

In this part of our study, we present the limitations of our CNN and CNN-LSTM models when applied to predicting the Channel Quality Indicator (CQI) in 4G LTE/5G mobile networks.

4.1.1. Limitations of the CNN Model

CNNs are effective at extracting local patterns from mobile network data, but they exhibit several limitations in the context of 4G LTE/5G mobile networks:

Focus on spatial rather than temporal features: CNNs primarily capture spatial or local characteristics but are not well-suited to modeling the temporal correlation between successive radio channel variables. However, CQI prediction strongly depends on the temporal evolution of the channel, which is influenced by fading, user mobility, and dynamic interference.

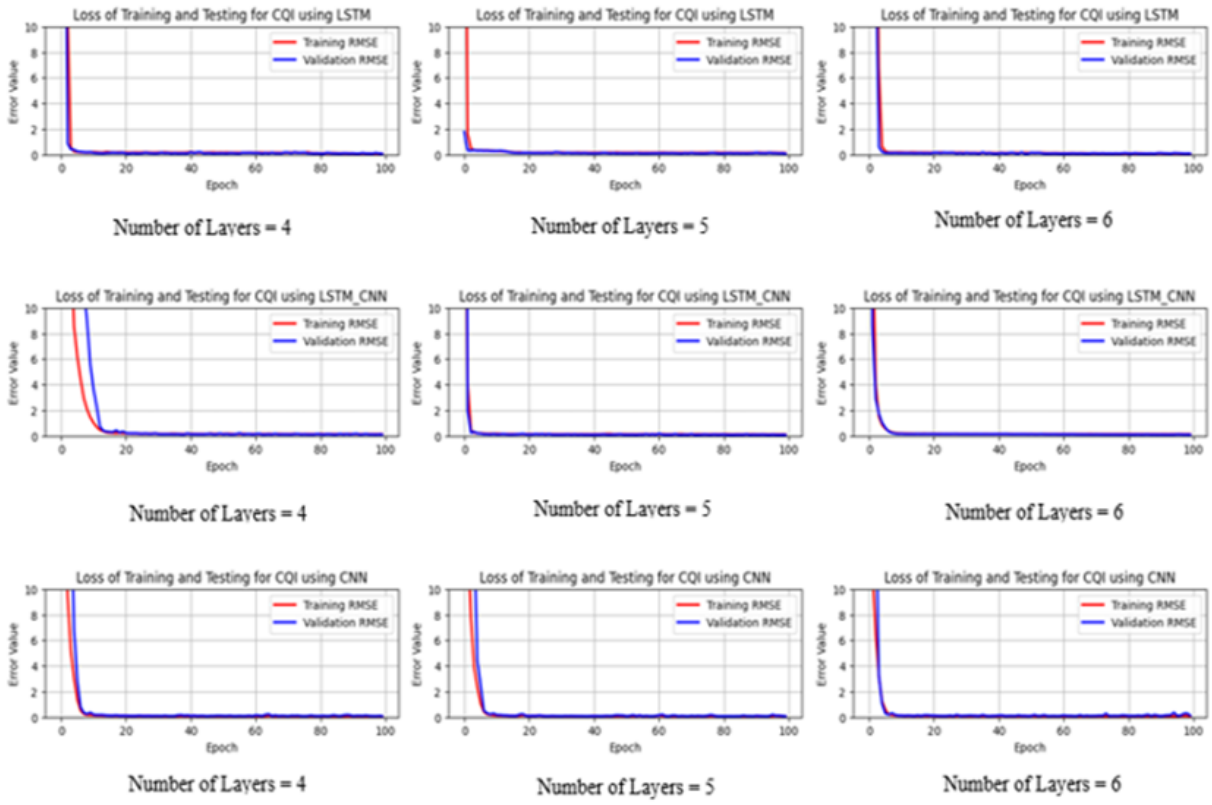

Fig. 11. Comparison of Training and Testing Data Losses Using RMSE.

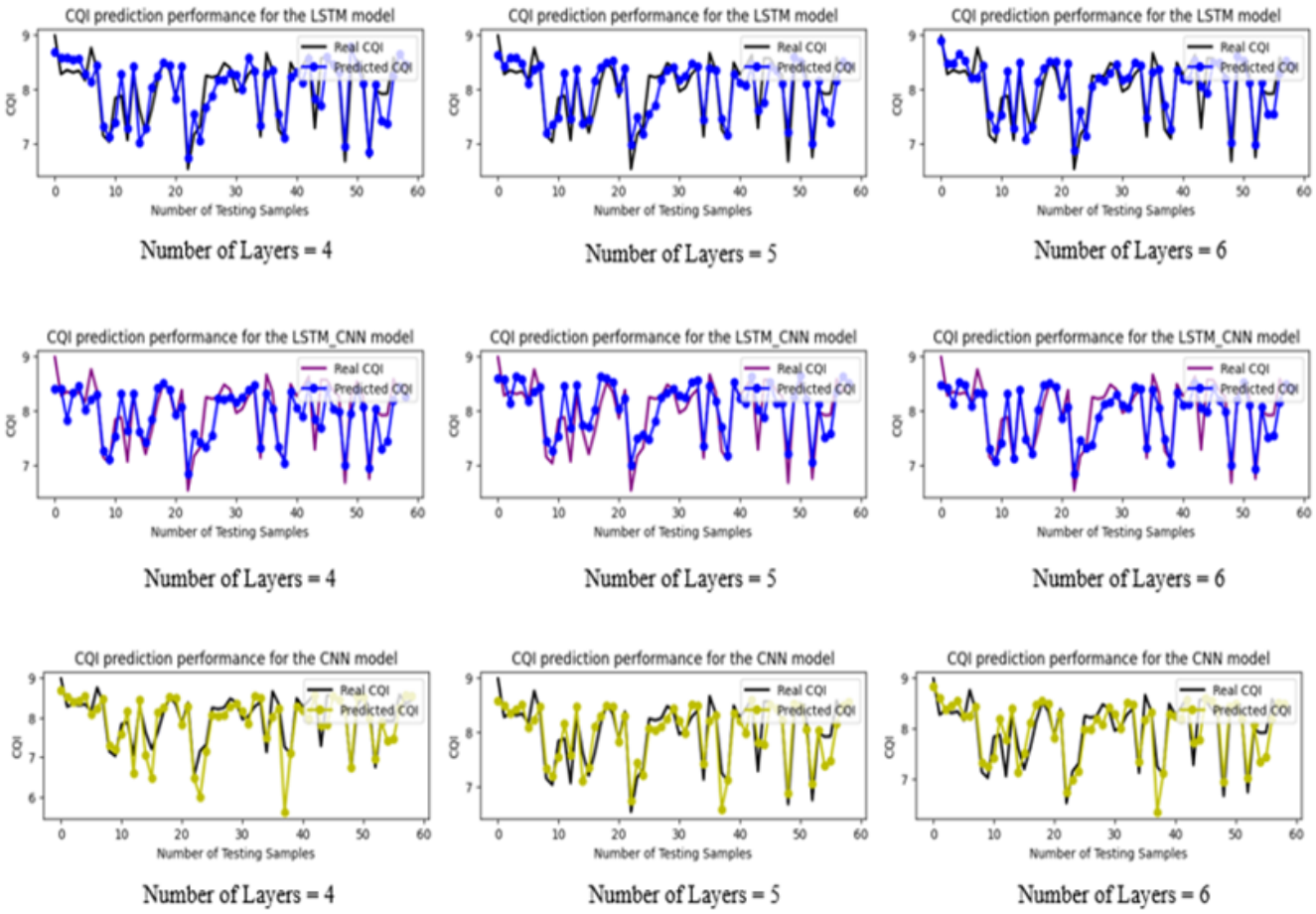

Fig. 12. Comparison of Actual and Predicted Values.

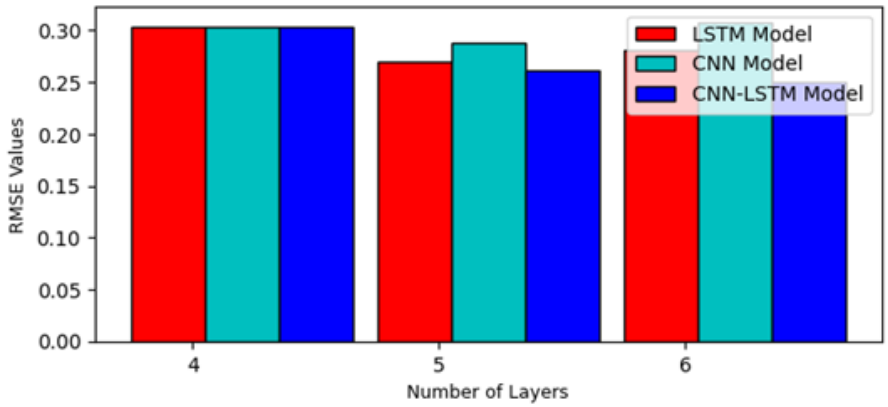

Fig. 13. Performance measurement using RMSE.

Difficulty handling high mobility scenarios: In 4G LTE/5G environments with high user mobility, the radio channel changes rapidly (e.g., Doppler effect, handover). Under such conditions, CNNs alone struggle to track these non-stationary variations effectively.

Data requirements and lack of interpretability: Training CNN models requires a large amount of diverse real-world data, which is often expensive for mobile operators to obtain. Like most deep learning models, CNNs also suffer from poor interpretability, making it difficult to explain how CQI predictions are generated. This limits their adoption by network engineers.

4.1.2. Limitations of the Hybrid CNN-LSTM Model

The hybrid CNN-LSTM model combines a CNN, which extracts local features, with an LSTM, which captures temporal dependencies. While the CNN-LSTM is more suitable than a standalone CNN, it also has notable limitations:

- The CNN + LSTM combination significantly increases the number of parameters, leading to longer training times and higher CPU (Central Processing Unit) / GPU (Graphics Processing Unit) resource consumption. As a result, the CNN-LSTM model is not always ideal for real-time deployment in a radio access network.

- The CNN-LSTM is highly sensitive to hyper-parameter selection (such as the number of LSTM layers and the learning rate). Poor tuning of these hyper-parameters can cause severe performance degradation.

- Given the heterogeneity of 4G LTE/5G networks, which consists of SBSs, MBSs, and multiple frequency bands, the CNN or CNN-LSTM models struggle to fully capture this complexity.

5. Conclusion

In this article, we extended our previous research [4] by introducing two new models, CNN and CNN-LSTM, for predicting CQI in 4G LTE/5G networks with SBSs. These models, trained and evaluated on real-world datasets collected from Orange Senegal's commercial 4G LTE/5G network, demonstrated strong predictive capabilities under realistic operating conditions. The results highlight the superiority of the hybrid CNN-LSTM architecture, which consistently outperformed both CNN and LSTM models, achieving the lowest RMSE (0.25).

This study's originality lies in combining CNN for local feature extraction with LSTM for temporal dependency modeling, effectively capturing complex spatio-temporal dynamics inherent in multi-band small cell deployments. By treating CQI as an ordinal continuous variable within a regression-discretization framework, our approach also offers a novel methodological contribution that enhances both accuracy and interpretability.

Beyond its technical performance, this work carries important practical implications. Accurate CQI prediction is critical for proactive resource allocation, adaptive modulation and coding, and energy-efficient management of mobile networks. Our findings confirm the potential of deep learning to enhance both quality of service (QoS) and spectral efficiency in heterogeneous and demanding environments.

Future research will extend this study toward real-time CQI prediction by integrating generative AI, reinforcement learning, and transfer learning, paving the way for autonomous and intelligent beyond-5G networks.

Availability of Data and Material

The datasets generated and/or analyzed during the current study are available from the corresponding author on reasonable request.

References

[1] C.V. Anamuro, A. Blanc, X. Lagrange, *Statistical analysis and characterization of signaling and user traffic of a commercial multi-band LTE system*, Telecommun Syst. 87 (2024) 437–453. https://doi.org/10.1007/s11235-024-01196-5

[2] L. Polak, J. Kufa, R. Sotner, T. Fryza, *Measurement and Analysis of 4G/5G Mobile Signal Coverage in a Heavy Industry Environment*, Sensors 24(8) (2024) 2538. https://doi.org/10.3390/s24082538

[3] N. Diouf, M. Ndong, D. Diop, K. Talla, A.C. Beye, I. Gueye, Finding Hidden Links among Variables in a Large-Scale 4G Mobile Traffic Network Dataset Using Machine Learning, 8th International Conference on Soft Computing & Machine Intelligence (ISCMI), Cairo, Egypt (2021) 1-8.
doi: 10.1109/ISCMI53840.2021.9654806

[4] N. Diouf, M. Ndong, D. Diop, K. Talla, M. Sarr, A.C. Beye, *Channel Quality Prediction in 5G LTE Small Cell Mobile Network Using Deep Learning*, 9th International Conference on Soft Computing & Machine Intelligence (ISCMI), Toronto, ON, Canada (2022) 15-20.
doi: 10.1109/ISCMI56532.2022.10068487

[5] S. Moon, H. Kim, I. Hwang, *Deep learning-based channel estimation and tracking for millimeter-wave vehicular communications*, Journal of Communications and Networks 22(3) (2020) 177-184.
https://doi:10.1109/JCN.2020.000012

[6] T.-H. Li, M.R.A. Khandaker, F. Tariq, K.-K. Wong, R. T. Khan, *Learning the Wireless V2I Channels Using Deep Neural Networks*, 2019 IEEE 90th Vehicular Technology Conference (VTC2019-Fall) (2019) 1-5.
https://doi:10.1109/VTCFall.2019.8891562

[7] L. Xiong, Z. Zhang, D. Yao, *A novel real-time channel prediction algorithm in high-speed scenario using convolutional neural network*, Wireless Netw 28 (2022) 621–634.
https://doi.org/10.1007/s11276-021-02849-y

[8] T. Ngo, B. Kelley, P. Rad, Deep Learning Based Prediction of Channel Profile for LTE and 5G Systems, European Wireless 2021; 26th European Wireless Conference, Verona, Italy (2021) 1-7.

[9] B. Sharma, V.S. Chaudhary, *Channel Estimation and Equalization Using FIM for MIMO-OFDM on Doubly Selective Faded Noisy Channels*, ECTI Transactions on Electrical Engineering, Electronics, and Communications 20(1) (2022) 74–82.
https://doi.org/10.37936/ecti-eec.2022201.246107

[10] S. Pahal, N. Rathee, B. Singh, *A Deep Learning-Based Model for Link Quality Estimation in Vehicular Networks*, IETE Journal of Researc, 69(8) (2021) 5159–5168.
https://doi.org/10.1080/03772063.2021.1973591

[11] K.K. Cwalina, P. Rajchowski, A. Olejniczak, O. Błaszkiewicz, R. Burczyk, *Channel State Estimation in LTE-Based Heterogeneous Networks Using Deep Learning*, Sensors 21(22) (2021) 7716.
https://doi.org/10.3390/s21227716

[12] R. Raj, A. Kulkarni, A. Seetharam, A. Ramesh, Wireless Channel Quality Prediction using Sparse Gaussian Conditional Random Fields, 18th Annual Consumer Communications, Networking Conference (CCNC), Las Vegas, NV, USA (2021) 1-6.
doi: 10.1109/CCNC49032.2021.9369651

[13] A.H. Jafari, D. López-Pérez, H. Song, H. Claussen, L. Ho, J. Zhang, *Small cell backhaul: challenges and prospective solutions*, EURASIP Journal on Wireless Communications and Networking 2015:206 (2015) 1-18.
https://doi.org/10.1186/s13638-015-0426-y

[14] J.M.H. Pinheiro, S.V.B. De Oliveira, T.H.S. Silva *et al.*, The Impact of Feature Scaling In Machine Learning: Effects on Regression and

Classification Tasks. arXiv preprint arXiv:2506.08274 (2025).

[15] H. Fu , S. Tang , X. Zhao, *Limitations of Correlation Coefficients in Research on Functional Connectomes and Psychological Processes*, Hum. Brain Mapp. 46(10) (2025) e70287. doi: 10.1002/hbm.70287. PMID: 40637219; PMCID: PMC12242859.

[16] A.S. AlSalehy, M. Bailey, *Improving Time Series Data Quality: Identifying Outliers and Handling Missing Values in a Multilocation Gas and Weather Dataset*, Smart Cities 8(3) (2025) 82. https://doi.org/10.3390/smartcities8030082.

[17] F. Ododo, N. Addotey, *Understanding the influence of outliers on machine learning model interpretability*, International Journal of African Sustainable Development Research 7(2) (2025) 41-58. https://doi.org/10.70382/tijasdr.v07i2.019

[18] A. Kulkarni, A. Seetharam, A. Ramesh, J.D. Herath, *DeepChannel: Wireless Channel Quality Prediction Using Deep Learning*, IEEE Transactions on Vehicular Technology 69(1)(2020) 443-456. https://doi:10.1109/TVT.2019.2949954

[19] T. Wang, C.-K. Wen, H. Wang, F. Gao, T. Jiang, S. Jin, *Deep learning for wireless physical layer: Opportunities and challenges*, China Communications 14(11) (2017) 92-111. doi: 10.1109/CC.2017.8233654

[20] K. Choudhary, B. DeCost, C. Chen, A. Jain, F. Tavazza, R. Cohn, *et al.*, *Recent advances and applications of deep learning methods in materials science*, npj Comput Mater 8(1) (2022) 59. https://doi.org/10.1038/s41524-022-00734-6

Appendix

Table A1
Data collection sample.

	Date	eNodeB Name	FT_DL_Traffic_4G_GB	FT_Traffic_4G_UL_GB	FT_Total_Traffic_4G_GB	FT_Active_user_4G_Max	FT_RRC_user_4G_Max	FT_throughput_4G_UL_user_KB	FT_Throughput_DL_user_Kb	FT_CDR_4G	FT_CQI_4G_Avg	FT_Radio_DL_Delay_avg_ms	DL_Perceived_Throughput_Mbits
2	2020-08-03	MASSALIK_P2	9,1122	2,7334	11,8456	6	21	6108,2071	12294,1876	0,0463	8,8456	48,1082	13,8656
3	2020-08-03	MASSALIK_P1	34,3516	4,4164	38,768	10	38	3371,2338	12788,9137	0,0502	8,2603	65,5873	13,6208
4	2020-08-03	MASSALIK_P4	6,4864	1,262	7,7484	6	25	3847,0465	13548,3103	0,0806	8,5026	26,0058	15,3909
5	2020-08-03	MASSALIK_P3	11,8418	1,5664	13,4081	6	34	3612,8278	15024,1367	0,1227	8,9841	36,9376	16,5974
6	2020-08-03	MASSALIK_P6	0,7508	0,228	0,9787	4	14	4330,5938	9341,5278	0,185	7,1185	23,9341	11,3655
7	2020-08-03	MASSALIK_P5	3,9212	0,2947	4,216	4	8	2061,9749	12668,0856	0,0363	7,4358	87,009	12,6886
8	2020-08-04	MASSALIK_P2	13,2907	2,5735	15,8642	7	30	4715,8309	13211,9078	0,1717	8,6488	75,5624	13,2149
9	2020-08-04	MASSALIK_P1	30,1341	3,8739	34,008	10	40	3136,9674	12904,2553	0,1114	8,195	48,4037	13,8162
10	2020-08-04	MASSALIK_P4	9,4402	1,0239	10,4642	7	27	2667,291	12459,3425	0,2773	8,7387	42,8907	13,8808
11	2020-08-04	MASSALIK_P3	10,2382	1,6246	11,8628	7	28	3407,6366	13961,4839	0,1913	8,8638	28,9928	16,0157
12	2020-08-04	MASSALIK_P6	1,5143	0,1927	1,707	4	13	2166,4826	9835,8311	0,2654	7,4868	54,8179	12,4538
13	2020-08-04	MASSALIK_P5	2,2437	0,8863	3,13	4	10	5166,589	10730,2363	0,1038	7,7112	24,8298	12,7797
14	2020-08-05	MASSALIK_P2	14,0649	3,0967	17,1617	8	24	5244,3826	13510,7352	0,3273	8,4301	67,3688	15,1057
15	2020-08-05	MASSALIK_P1	33,3411	4,8187	38,1598	11	41	3082,89	12356,7202	0,1518	8,3494	65,7874	12,7549
16	2020-08-05	MASSALIK_P4	10,8806	1,3496	12,2302	7	27	2991,9169	12604,2744	0,171	8,3422	39,2042	13,5282
17	2020-08-05	MASSALIK_P3	12,33	1,2008	13,5308	7	30	2356,6425	13003,9303	0,2786	8,645	52,3123	14,2949
18	2020-08-05	MASSALIK_P6	1,2564	0,2536	1,51	4	10	3138,1601	9597,7531	0,1414	7,3189	27,9292	12,0078
19	2020-08-05	MASSALIK_P5	4,403	0,7009	5,1039	5	14	2649,8213	10731,7426	0,3703	7,6683	29,397	12,6883
20	2020-08-06	MASSALIK_P2	35,6651	2,4289	38,094	9	27	3168,5863	18888,534	0,2871	8,5342	96,737	20,3315
21	2020-08-06	MASSALIK_P1	33,9944	3,4409	37,4353	10	46	2994,3761	13556,2239	0,1339	8,2334	67,2189	14,1869
22	2020-08-06	MASSALIK_P4	12,8526	1,6335	14,4861	6	27	3104,2256	13960,4399	0,2347	8,5436	42,9225	15,3308
23	2020-08-06	MASSALIK_P3	15,0554	1,5529	16,6083	7	36	2662,4233	13184,6945	0,304	8,5152	38,0817	14,0724
24	2020-08-06	MASSALIK_P6	1,055	0,1213	1,1763	4	11	1609,9028	7437,0016	0,2428	7,1266	37,2296	10,2504
25	2020-08-06	MASSALIK_P5	7,5542	1,3095	8,8637	5	14	2527,9551	11052,0348	0,3258	7,5431	13,8654	11,3656
26	2020-08-07	MASSALIK_P2	20,2818	2,5307	22,8125	8	101	3847,4616	16166,4908	0,2556	8,5169	61,9166	17,6734